Desalination and Water Treatment
www.deswater.com

doi: 10.5004/dwt.2018.22300

113 (2018) 335–345
May

Sorption of tribromophenol with magnetic ion exchange resin: Isotherm, kinetics, and thermodynamics

Yulin Tang[a,c], Qianhong Liu[a], Yong He[a,b], Minkang Tang[b], Anqi Li[a], Jianwei Fan[a,*]

[a]*State Key Laboratory of Pollution Control and Resources Reuse, College of Environmental Science and Engineering, Tongji University, Shanghai, 200092, China, Tel. +86 21 65982658, email: fanjianwei@tongji.edu.cn*
[b]*School of Resources and Environment Engineering, Jiangxi University of Science and Technology, Ganzhou, 341000, China*
[c]*Shanghai Institute of Pollution Control and Ecological Security, Shanghai, 200092, China*

Received 19 October 2017; Accepted 1 April 2018

ABSTRACT

The use of magnetic ion exchange (MIEX) resin as an efficient adsorbent in the removal of tribromophenol (TBP) was investigated by batch and column experiments in this study. The influences of contact time, initial TBP concentration, pH, coexisting matters and temperature on the sorption of TBP were determined. The adsorption mechanism was also demonstrated. The sorption kinetics could be well fitted by the pseudo-second-order model. The removal of TBP was high at pH = 7.80, the sorption rate increased when increasing the initial pH from 3.59 to 7.80 and sharply decreased with the initial pH increasing from 7.80 to 10.85. The capacity of major anions to reduce TBP sorption followed the order of $SO_4^{2-} > HPO_4^{2-} > HCO_3^- > NO_3^-$. As for cations, $Mg^{2+} > Ca^{2+} > NH_4^+$. The results showed that the maximum sorption capacity was 72.24 mg/g with the Langmuir model and the sorption equilibrium agreed with Freundlich isotherm. The hydrophobic interaction of the benzene ring and hydrogen bonds might be responsible for the sorption of TBP on MIEX. The procedure of TBP sorption was a thermodynamically spontaneous and endothermic process according to the negative ΔG^0, positive ΔH^0 and positive ΔS^0 values. The breakthrough curve was successfully fitted by the Thomas and Yoon-Nelson model. After the statics and dynamics statistics, the MIEX was proven to be a good option for the removal of TBP.

Keywords: TBP; MIEX resin; Sorption; Kinetics; Thermodynamics; Column test

1. Introduction

As a representative of flame retardants, brominated flame retardants (BFRs) are one of the largest and the most frequently used groups on the market, due to their high performance and low cost [1,2]. The impacts of BFRs on the environment and human health and the proliferation of BFRs in the environment have been investigated in previous studies [3,4]. Tribromophenol (TBP) is a relatively persistent compound among BFRs, and it was incorporated into the list of hazardous wastes by the Environmental Protection Agency in 1998 [5]. As a kind of halogenated phenolic compound, TBP is generally found in consumer products, including telephones, refrigerators, packaging materials and so on [6]. TBP is also used to treat timber as fungicide [3,7]. Because of the extensive use of TBP, it can be widely found in soil, landfill leachate and sewage sludge [8]. TBP has great endocrine-disrupting potencies which are the causes for growing concern in scientific communities and governmental agencies. According to previous researches, TBP has bioaccumulation in human placenta tissues, so it can result in fetal BFRs exposure during pregnancy process [9,10]. Unfortunately, the manufacture yield of TBP was estimated to be approximately 9500 t/y worldwide in 2001, and TBP is commonly found in extremely high concentrations in the environment [11,12].

Several serviceable techniques, such as oxidation, biodegradation and adsorption have been explored for the removal of TBP from water [13–21]. The uncomplicated and

*Corresponding author.

high efficiency of various adsorbents, including core-shell nanoparticles, porous materials, sawdust and chalk, have been investigated in previous studies [22–24]. It is reported that anion exchange resin has great adsorption capacity to both natural organic matters and bromides [25,26]. Recently, magnetic ion exchange resin has been proven to be a very promising material in water treatment to remove organic matter such as bentazone, 2-methylisoborneol and geosmin [27–29].

MIEX resin was developed jointly by Orica Watercare, Commonwealth Scientific Industrial Research Organization and South Australian Water Corporation [30]. It has general properties of anion exchange resin, such as a polyacrylic matrix in the chloride form, a macroporous structure, strong-base functional groups, and medium pore size and porosity [30,31]. Compared with traditional anion exchange resins, MIEX resin has two specific characteristics. Firstly, it has magnetized iron oxide incorporated into the structure, which aids agglomeration and settlement. Secondly, MIEX resin has a relatively small particle size of 150–180 μm, which is 2–5 times smaller than other traditional resins, providing much greater external surface area [32,33]. According to previous studies, the specific surface of MIEX is 21.47 m^2/g, and the mean pore diameter is 16.96 nm. This high surface area of MIEX resin leads to a fast ion exchange kinetics [34]. Due to its excellent magnetic characteristic, MIEX can be easily separated from water after adsorption [35–37]. However, less research has reported the TBP removal characteristics from water by MIEX. It is necessary to investigate the different influencing factors of TBP adsorption on MIEX in batch tests and it is also essential to evaluate the dynamic sorption performance and characteristics by column test.

The overall objective of this study was to scientifically evaluate the removal behaviors of TBP on MIEX from aqueous solution. The effects of contact time, initial TBP concentration, pH, coexisting anions, coexisting cations, coexisting organic matters and temperature were investigated in batch tests. The adsorption kinetics under various operating conditions were taken into consideration. The equilibrium isotherm curve was fitted by the Langmuir, Freundlich and Temkin isotherm models. In addition, the sorption kinetics was fitted by the pseudo-first-order model and the pseudo-second-order model. The thermodynamics parameters including the free energy, enthalpy and entropy were also calculated and discussed. Besides, The breakthrough curve for the dynamic adsorption of TBP on fixed-bed column with MIEX was carried out systematically, and three models were used to fit the breakthrough curve. The results provided an outstanding comprehension of the sorption process of TBP on MIEX, which developed an available and promising method for water treatment.

2. Materials and methods

2.1. Materials and reagents

The MIEX resin was purchased from the China Agent of Orica Watercare of Victoria, which was washed three times by Millipore deionized water (DI water) to remove impurity substances before being used. Scanning electron microscopy (SEM) results were obtained from a TESCAN (Vega3XMU) to observe the surface morphology of the MIEX resin.

TBP and Methanol (HPLC grade) were obtained from Tanso Company (Shanghai, China). All other reagents used in this study were reagent grade and supplied by Sinopharm Chemical Reagent (Shanghai, China). The stock solutions of TBP, sulfate, carbonate, phosphate, and nitrate were prepared respectively using their sodium salts, and the stock solutions of ammonium, calcium and magnesium were prepared using their sulphate salts. The standard stock solution of TBP was diluted into various concentrations if necessary. All the solutions throughout the experiments were prepared by DI water.

2.2. Experimental procedures

2.2.1. Batch sorption isotherm tests

For batch sorption isotherm tests, 0.05 mL MIEX and 200 mL TBP solution with selected concentrations were dispersed in 250 mL capped glass tubes. These tubes were transferred into an incubator and shaken at 150 rpm and 298 K. The MIEX was then magnetically separated from the suspension and the TBP concentration was measured. After 24 h, the solution samples were taken out and filtered by 0.45 μm membrane before analysis. All the experiments were carried out in triplicate.

2.2.2. Kinetic tests

For batch kinetic tests, the experiments were carried out in 250 mL capped glass tubes containing 0.05 mL MIEX and 200 mL TBP solution with two different initial concentrations (1.0 mg/L and 2.0 mg/L). In each test, the glass tubes were transferred into an incubator as before and shaken at 150 rpm and 298 K for 24 h. Then 2 mL samples were taken out and filtered by 0.45 μm membrane for analysis at predetermined time intervals.

2.2.3. Independent variable tests

Independent variable tests were carried out to investigate the effect of initial solution pH (4.0–11.0) and temperature (288.0 K–308.0 K) on TBP sorption. The pH and temperature were varied within a certain range while other solution parameters were kept constant. Stock NaOH or HCl solution were used to adjust the initial pH of each solution to the predetermined pH value. The detailed experimental procedures were similar to the batch sorption isotherm tests.

2.2.4. Effect of coexisting matter

The effect of coexisting anions on the sorption of TBP on MIEX resin was investigated by adding a certain amount of NO_3^-, SO_4^{2-}, HCO_3^- and HPO_4^{2-} stock solution to each test tube to reach a preselected concentration. As for coexisting cations, certain cation stock solutions, including NH_4^+, Ca^{2+} and Mg^{2+} were added to each test tube the same way. For the impact of coexisting organic matter, certain amount of humic acid (HA) was added to each tube at target concentrations ranging from 0.0 to 30.0 mg/L. The initial concentration of TBP was 2.0 mg/L in all the experiments and the detailed experimental procedures were similar to the batch sorption isotherm tests.

2.2.5. Fixed-bed column tests

Fixed-bed column tests were carried out to explore the dynamic removal of TBP from water by MIEX. An acrylic column with 1.0 cm in diameter and 6.0 cm in height was used in the MIEX resin-sand system. A 0.4 cm layer of MIEX resin was put above a 0.5 cm layer of sand in the column. The flow rate was monitored by a vacuum pump, which was connected to the top of the column. In addition, 50 μm membranes were placed at the inlet and outlet of the fixed-bed column to distribute the water flow over the cross-sectional area of the column. DI water was injected into the column for 2 h after packing the column. The TBP solution was continuously injected into the column with a flow rate of 1.0 mL/min and the effluent samples were collected at preselected time interval of 30 min. The concentration of TBP in effluent was measured with liquid chromatography and the breakthrough curve was fitted by three models. When the effluent concentration of TBP equaled to the initial concentration, is was indicated that the fixed-bed column test was terminated.

2.3. Analytical methods

The concentration of TBP was determined by liquid chromatography (LC-2030, Shimadzu corporation, Japan) with a reversed phase C18 column (250 mm × 4.6 mm × 5 μm, VP-ODS). TBP was measured in a partial pressure grade with methanol/water as mobile phase. The flow rate of certain solution was kept at 1.0 mL/min and the injection volume was 20 μL. The detection wavelength was 218 nm and the temperature of the column was 308 K. The solution pH were measured using a pH meter (Mettler Toledo). All experiments were carried out in triplicate.

2.4. Mathematical equations and models

2.4.1. Calculations

The TBP uptake on MIEX can be calculated according to Eq. (1).

$$q_t = \frac{(C_0 - C_t)V}{m} \tag{1}$$

where q_t (mg/g) represents the adsorbed amount of TBP at time t, C_0 and C_t (mg/L) represent the initial liquid-phase concentration and liquid-phase concentration at time t, respectively. V (L) means the solution volume, and m (g) represents the mass of MIEX.

Thermodynamics analysis will illustrate the sorption characteristics of TBP on MIEX resin from the aspect of energy change. The following Eqs.(2), (3) can be used to calculate the thermodynamic parameters, containing standard enthalpy change (ΔH^0, kJ/mol), standard entropy change (ΔS^0, J/mol K) and standard Gibbs free energy change (ΔG^0, kJ/mol).

$$lnKD = \frac{\Delta S^0}{R} - \frac{\Delta H^0}{RT} \tag{2}$$

$$\Delta G^0 = \Delta H^0 - T\Delta S^0 \tag{3}$$

where K_D (L/mL) is the distribution coefficient; R (8.314 J/mol K) is universal gas constant and T (K) is the temperature.

Fixed-bed column tests were carried out to explore the maximum absorbed amount of TBP on MIEX, which can be calculated by Eqs.(4)–(6).

$$m = v\int_0^{t2} C_t d_t \tag{4}$$

$$m_0 = vt_2C_0 \tag{5}$$

$$S = \frac{m_0 - m_{eff}}{w} \tag{6}$$

where t_2 is the time for sorption equilibrium (h), v is the flow rate (mL/min), m_{eff} is the mass of effluent TBP (mg), m_0 is the total mass of TBP passed through the column (mg), S is the saturation capacity of the dynamic sorption (mg/g), w is the weight of the MIEX (g).

2.4.2. Kinetic models

Sorption kinetics reflects the removal efficacy of adsorbate on adsorbent as time elapsing. It is essential for understanding the mechanisms of adsorption. Two kinetic models, pseudo-first-order and pseudo-second-order model, were used to fit the experimental data, which can be expressed by Eqs. (7), (8).

$$\text{pseudo-first-order model}: ln(q_e - q_t) = lnq_e - k_1t \tag{7}$$

$$\text{pseudo-second-order model}: \frac{t}{q_t} = \frac{1}{k_2q_e^{\,2}} + \frac{1}{q_e}t \tag{8}$$

where k_1 and k_2 are the rate constants of the two models, respectively, h_0 is the initial sorption rate, which can be determined from the equation .

2.4.3. Isotherm models

The sorption process will reach equilibrium at a certain temperature. The sorption isotherm is a relationship curve that describes TBP sorption equilibrium characteristics. The sorption isotherm is crucial and useful, it usually gives some insights into the sorption mechanism, surface properties and affinity of adsorption. We can get lots of information from it, such as comparing the sorption characteristics with different adsorbents, elucidating the adsorption state on adsorbent surface and even calculating adsorption parameters. The isotherm experimental data was further fitted by Langmuir, Freundlich and Temkin isotherm models, including: Eqs. (9)–(11).

$$Langmuir: \frac{C_e}{q_e} = \frac{C_e}{q_{max}} + \frac{1}{q_{max}b} \tag{9}$$

$$\text{Freundlich}: logq_e = \frac{logC_e}{n} + logk_f \tag{10}$$

$$\text{Temkin: } q_e = BlnC_e + BlnA \tag{11}$$

where q_e (mg/g) is TBP adsorption capacity at equilibrium concentration, C_e (mg/L), and q_{max} (mg/g) is the maximum adsorption capacity, b is the Langmuir model constant, while n and k_f are the Freundlich model constants. A and B are the Temkin model constants. Correlation coefficient (R^2) was used to assess the validity of each isotherm models.

2.4.4. Breakthrough curve models

Three breakthrough curve models, the Thomas model, the Yoon-Nelson model and the Clark model, were used to fit the breakthrough curve, which can be expressed by Eqs. (12)–(16). The Thomas model, which follows the Langmuir kinetics of adsorption-desorption, is one of the most generally used models in describing column performance and predicting breakthrough curves. It assumes that the axial dispersion in the column adsorption is negligible, since the rate driving force obeys the second-order reversible kinetics [38,39]. The Yoon-Nelson model is based on the suppose that the decrease rate which is in the possibility of each adsorbate molecule, is proportional to the possibility of adsorbate adsorption and the adsorbate breakthrough [40, 41]. The Clark model assumes that the sorption behaviour of adsorbates follows the Freundlich adsorption isotherm, and the external mass transfer step determines the sorption rate [42].

$$\text{Thomas: } Z_0 = \frac{F}{K_a N_0} ln\left(\frac{C_0}{C_B} - 1\right) \tag{12}$$

$$ln\left(\frac{C_0}{C_t} - 1\right) = \frac{k_{THq0} M}{Q} - k_{TH} C_0 t \tag{13}$$

$$\text{Yoon-Nelson: } t = T + \frac{1}{k'T} ln\left(\frac{C_t}{C_0 - C_t}\right) \tag{14}$$

$$K = K' \cdot T \tag{15}$$

$$\text{Clark: } ln\left[\left(\frac{C0}{C}\right)^{n-1} - 1\right] = lnA - rt \tag{16}$$

where Z_0 is the critical bed depth, where a plot of $\ln[C_0/C_t - 1]$ against t gives a straight line from which the values of k_{TH} and q_0 are determined from the intercept and the slope. K is the proportionality constant, where a plot of $\ln[C_0/C_t - 1]$ against t gives a straight line from which the values of K' and T are determined from the intercept and the slope. A and r are determined from the slope and the intercept of plots of $\ln((C_0/C)^{n-1} - 1)$ versus t.

3. Results and discussion

3.1. Sorption kinetic studies

3.1.1. Effect of contact time and initial TBP concentration

The sorption of TBP on MIEX was investigated as a function of contact time at two different initial TBP concentrations (1.0 and 2.0 mg/L). The water samples were taken at preconcerted time intervals of 5, 10, 30, 60, 90, 120, 180, 240, 300, 600, 900, 1200 and 1440 min. A smooth curve leading to the adsorption equilibrium of TBP is shown in Fig. 1. According to Fig. 1, the TBP removal increased with the contact time increasing. The uptake of TBP on MIEX dramatically increased within initial 300 min, then the uptake slowly increased as time elapsed from 300 to 600 min and there was no significant change after 600 min. It is clear to say that the sorption process of TBP on MIEX resin reached equilibrium within 600 min in this study. There are several causes for this phenomenon. Firstly, the number of accessible vacant surface exchange sites is enough for TBP at the beginning of sorption, and the possibilities of interaction between the sorption sites and TBP molecule are greater in higher initial concentration, which is necessary to adsorption occurrence. As sorption process continues, these sorption sites are occupied by TBP and it is more difficult for the occupation of remaining sites due to the repulsive forces between the TBP molecules and MIEX [43]. Secondly, high TBP concentration solution has greater concentration gradient which results in the TBP adsorbed on the surface of MIEX migrating into the pores. It may provide additional sites for adsorption of more TBP. As for the sorption of other pollutants onto MIEX, the trend was similar [44].

3.1.2. Modeling of sorption kinetics

Two kinetic models were used to determine the sorption mechanism of TBP on MIEX resin at two different initial TBP concentrations and potential rate controlling steps. The data of the experiment were fitted by the pseudo-first-order model and the pseudo-second-order model according to Eqs. (7), (8) respectively, and the fitting results are listed in Table 1. The values of correlation coefficients for the pseudo-second-order model were higher than those of the pseudo-first-order model, which reveals that the pseudo-second-order model can fit the sorption of TBP on MIEX resin well. The pseudo-second-order model is based

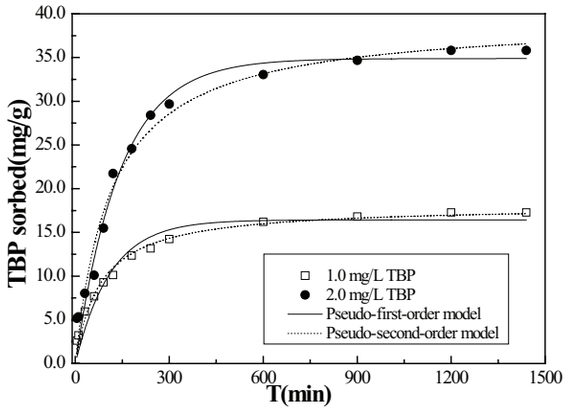

Fig. 1. Effect of contact time and initial concentration on TBP sorption (MIEX = 0.25 mL/L; shake speed = 150 rpm; pH = 7.80; temperature = 298 K).

on the assumption that chemical sorption is the rate-limiting step, containing covalent forces through sharing or exchanging of electrons between the MIEX resin and TBP [45–47]. Therefore, we can perorate that the sorption process of TBP on MIEX is a chemical sorption process. Additionally, the equilibrium sorption capacities ($q_{e,cal}$) calculated from the pseudo-second-order model at two different initial TBP concentrations were 18.07 and 39.48 mg/g respectively, which were close to the experimental results ($q_{e,exp}$). As shown in Table 1, with the initial TBP concentration of 1.0 and 2.0 mg/L, the initial sorption rate h_0 obtained from the pseudo-second-order model increases from 0.23 to 0.34. This phenomenon may be explained by the fact that the concentration gradient between the liquid and solid phase can be elevated in higher initial TBP concentration, leading to the increase in sorption driving force [48].

3.2. Effect of pH

As shown in Fig. 2a, the influence of pH on the sorption of TBP on MIEX resin was investigated with the initial pH value ranging from 3.59 to 10.85. It is indicated that pH is an important influencing factor on the sorption of TBP on MIEX resin and the sorption capacity is relatively high at pH = 7.80. The uptake of TBP increased from 20.80 mg/g to 34.30 mg/g when increasing the initial pH from 3.59 to 7.80, and sharply decreased from 34.30 mg/g to 22.32 mg/g when increasing the initial pH from 7.80 to 10.85. Competing adsorption of chloride and hydroxide ions introduced by hydrochloric acid and sodium hydroxide, which were used to adjust various pH values of the solution, may lead to the dependence of MIEX on pH value [49]. In the ionization of TBP, an H^+ proton is released from the phenolic group: TBP → TBP^- + H^+ , the TBP and TBP^- distribution fraction in water are shown in Fig. 2b [50]. TBP has a proton-binding site, carboxyl group with pKa value of 7.5. When the pH value exceeds 7.5, TBP exists mainly in the form of TBP^-, while the electrostatic repulsion between the net negatively charged MIEX and phenoxy anions results in a decrease of sorption [51]. Furthermore, TBP can form a complex with sodium ions when the pH value was above 10, so there was less TBP uptake by MIEX resin in high pH [50]. In consideration of the pH value of natural water bodies generally varies from 6.0 to 9.0, the high removal rate of TBP on MIEX resin in the wide pH range proves that the MIEX resin is appropriate to apply in removal of TBP from natural water bodies.

3.3. Effect of coexisting anions and cations

A variety of inorganic cations and anions are generally present in natural water bodies. In this study, the impacts of different anions, including NO_3^-, SO_4^{2-}, HCO_3^- and HPO_4^{2-}, different cations, including NH_4^+, Ca^{2+}, and Mg^{2+}, on TBP

Table 1
Fitting parameters of TBP sorption on MIEX resin using the pseudo-first-order and the pseudo-second-order kinetics model

C_0 (mg/L)	$q_{e,exp}$ (mg/g)	Pseudo-first-order model			Pseudo-second-order model		
		$q_{e,cal}$ (mg/g)	K_1 (mg/g min)	R^2	$q_{e,cal}$ (mg/g)	K_2 (mg/g min)	R^2
1.0	17.29	16.43	0.0089	0.941	18.07	7.04 10^{-4}	0.980
2.0	35.82	34.89	0.0070	0.975	39.48	2.21 10^{-4}	0.975

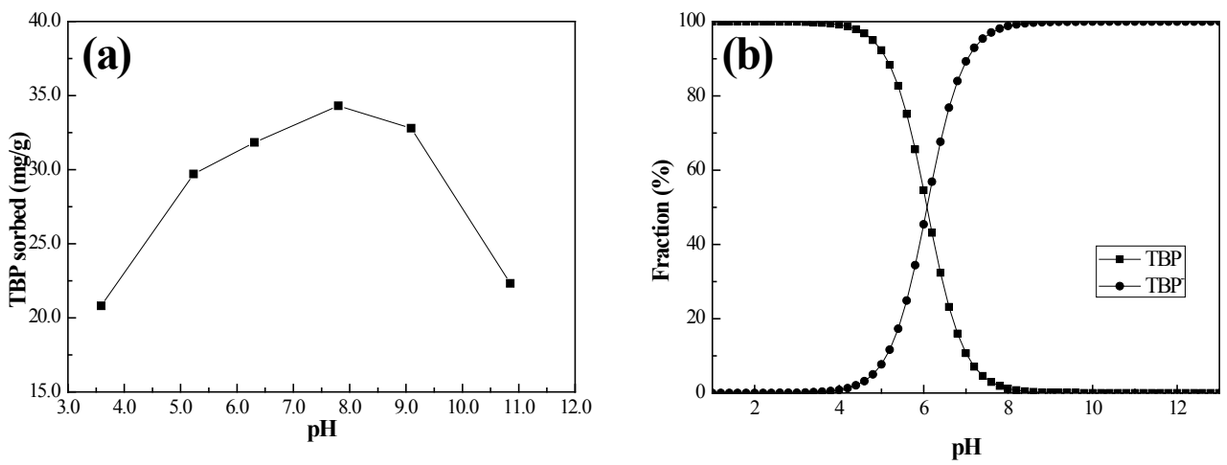

Fig. 2. (a) Effect of pH on TBP sorption (MIEX = 0.25 mL/L; T = 298 K; TBP = 2.0 mg/L). (b) The species distribution of TBP in water among the whole pH range.

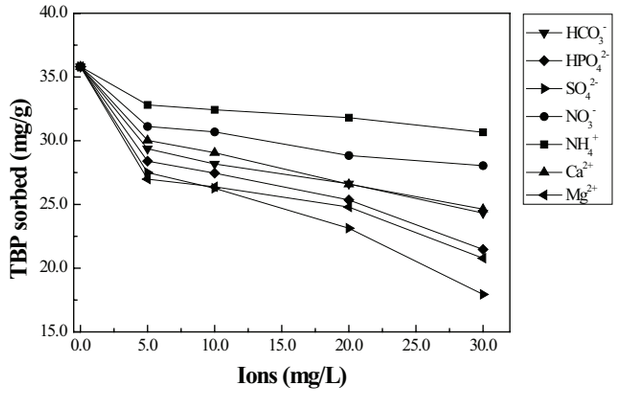

Fig. 3. Effect of major anions and cations on TBP sorption (MIEX = 0.25 mL/L; T = 298 K; TBP = 2.0 mg/L; pH = 7.80).

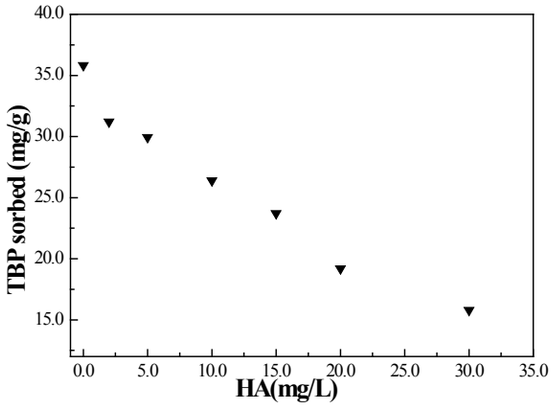

Fig. 4. Effect of coexisting HA on TBP sorption (MIEX = 0.25 mL/L; T = 298 K; TBP = 2.0 mg/L; pH = 7.80).

removal were carried out at the pH value of 7.80 and the results are shown in Fig.3. The concentrations of these anions and cations varied from 0.0 to 30.0 mg/L, whereas the initial concentration of TBP was 2.0 mg/L in all the experiments. As shown in Fig. 3, the inhibitions of NO_3^-, HCO_3^- and NH_4^+ were not significant even at very high concentrations (30.0 mg/L), they had little inhibition on TBP sorption on MIEX in this study. Meanwhile, the presence of SO_4^{2-}, HPO_4^{2-}, Ca^{2+} and Mg^{2+} could drastically decrease TBP removal and SO_4^{2-} and Mg^{2+} had stronger inhibition. The impacting level that different types of anions have on TBP removal followed the sequence: $SO_4^{2-} > HPO_4^{2-} > HCO_3^- > NO_3^-$. The results of cations could be represented by the order: $Mg^{2+} > Ca^{2+} > NH_4^+$. The SO_4^{2-}, HPO_4^{2-}, Ca^{2+} and Mg^{2+} ions are competing ions for the adsorption of TBP. This phenomenon could be explained by the competition between different types of anions or cations and TBP for the active sorption sites on the MIEX surface [52,53].

3.4. Effect of natural organic matter

Natural organic matter (NOM) is generally appearing in natural water body, which has a significant effect on water quality. Humic acid (HA) is one of the representative of naturally occurring macromolecular organic matter, which exists in surface water and groundwater ubiquitously, and plays an important role in the leaching, translating and degrading of organic pollutants. According to the structure of HA, a large amount of quinines and phenolic moieties exist, and the competition for oxidative species is the main cause for the inhibition of HA [54]. In this study, the effect of HA on TBP removal was determined by varying HA concentration from 0.0 to 30 mg/L. In all the experiments, the initial TBP concentration was 2.0 mg/L and the initial pH was 7.80. As shown in Fig. 4, the TBP uptake decreased from 35.75 to 15.79 mg/g while the concentration of HA increased from 0.0 to 30.0 mg/L. The results indicated that HA had an obvious effect on the removal of TBP on MIEX resin. The competition of HA and TBP for sorption sites resulted in reducing the TBP sorption on MIEX resin.

3.5. Sorption thermodynamics studies

3.5.1. Effect of temperature

Fig. 5 illustrates the effect of temperature on TBP removal by the MIEX resin, which was investigated by varying the temperature of solution from 288 to 308 K. It can be seen from Fig. 5 that TBP sorption on MIEX increased as the temperature increased. The maximum amount of TBP adsorbed slightly increased from 65.16 to 69.66 mg/g with temperature increasing from 288 to 308 K. This phenomenon indicated that the temperature of solution has certain effect on TBP removal, and the sorption of TBP on MIEX resin was an endothermic process in nature. This indicates that MIEX can be used to remove TBP in a certain range of temperature raw water, it can be used not only in summer but also in winter. It is well known that the solution viscosity decreases with temperature increasing, which permits the improved diffusion of TBP across the external boundary layer and in the internal pores of the MIEX resins. The sorption capacity relatively highly increased at higher temperature, it may be partly resulted from its greater external surface area and smaller particle size [44,55].

3.5.2. Sorption isotherm

The sorption isotherm can conveniently present the relationship between equilibrium concentration and equilibrium adsorption capacity at certain temperature. The sorption isotherm usually provides some insight into the sorption mechanism, surface properties and affinity to adsorbent. Three adsorption isotherm models, Langmuir, Freundlich and Temkin model, were used to fit the sorption equilibrium data and the fitted constants for the three models are listed in Table 2. The results of the adsorption equilibrium of TBP on MIEX resin at three temperatures are given in Fig. 5. The Langmuir model is based on perfect adsorbent surface and monolayer sorption on specific homogenous sites, meanwhile, the Freundlich model represents sorption process on heterogeneous surfaces [56,57]. The Temkin model reflects the effects of indirect interactions among

Table 2
Isotherm parameters for TBP sorption on MIEX resin

T(K)	Langmuir			Freundlich			Temkin		
	q_m (mg/g)	b (L/mg)	R^2	k_f	n	R^2	A	B	R^2
288	68.72	6.02	0.884	62.26	2.80	0.992	105.31	12.68	0.937
298	72.24	6.26	0.909	67.51	2.69	0.995	96.83	13.76	0.947
308	75.49	6.53	0.927	72.78	2.61	0.991	91.57	14.78	0.951

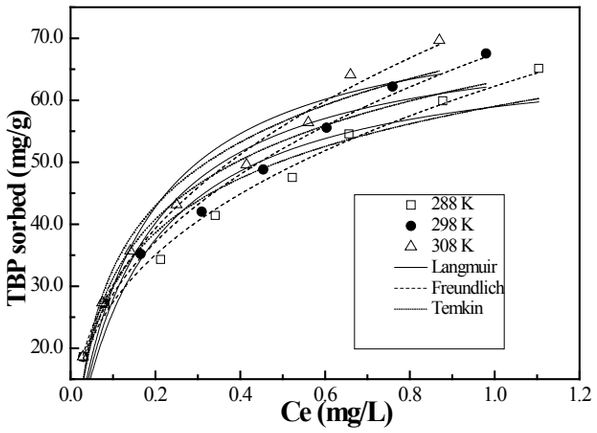

Fig. 5. Sorption isotherms of TBP on MIEX at different temperatures (MIEX = 0.25 mL/L; pH = 7.80). The solid lines represent non-linear curve fitting by Langmuir model; the dash lines represent non-linear curve fitting by Freundlich model; the dot lines are the curve fitting by Temkin model.

adsorbates during the sorption process [58]. As shown in Table 2, the maximum sorption capacity is 72.24 mg/g based on the Langmuir model. However, the sorption isotherm of TBP could be fitted better by the Freundlich model with the higher correlation coefficient values (R^2 > 0.980).

3.5.3. Sorption thermodynamics

Eqs. (2), (3) were used to calculate the values of the Gibbs free energy change ΔG^0, the enthalpy change ΔH^0, and the entropy change ΔS^0 for the sorption of TBP on MIEX resin at different temperatures and the results are shown in Table 3. In this study, the ΔG^0 values were negative at all temperatures, which indicated that the sorption of TBP on MIEX resin was spontaneous. Meanwhile, with the temperature increasing from 288 K to 308 K, the values of ΔG^0 were similar to each other, showing that the removal of TBP on MIEX resin was independent of the temperature. The ΔH^0 values were found to be positive, implying that during the sorption the heat was absorbed, which proved the sorption of TBP on MIEX resin was an endothermic process, so the rise in temperature does favor to the adsorption process. In addition, the positive value of ΔS^0 demonstrated the increased in randomness at the solid/liquid interface after sorption.

Table 3
Thermodynamic parameters of TBP sorption on MIEX resin

Thermodynamic constant	T (K)		
	288	298	308
ΔG^0 (kJ/mol)	–13.913	–14.499	–15.087
ΔH^0 (kJ/mol)		2.996	
ΔS^0 (J/mol K)		58.712	

3.6. Column test

Gupta has proposed the primary sorption zone (PAZ) concept, which could be used to analyze the breakthrough data of TBP adsorption on MIEX resin in the fixed-bed columns. The PAZ formed as a narrow band during the TBP injected into the fixed-bed initially. With the column test continued, the upper layers of MIEX resin became saturated and the PAZ advanced downward through the column until it reached the bottom of the column. At that moment, the column began to be broken [59,60].

The breakthrough curves and the fitted results used three different models following Eqs. (12)–(16) are shown in Fig. 6 and Table 4. As shown in Table 4, due to the higher correlation coefficient values, the breakthrough curve of TBP could be fitted better by the Yoon-Nelson model and Thomas model than the Clark model. According to the above equations, the maximum amount of TBP adsorbed on MIEX were 32.11 mg/g [61]. Because the adsorbent at the bottom of the column could not play the same role as the adsorbent at the top of the column, the dynamic sorption saturation capacity of TBP on MIEX was less than the static sorption capacity, 35.75 mg/g. According to the fixed-bed column test, MIEX was still indicated to have a high sorption capacity for TBP removal, so it came to the decision that MIEX could be an efficient and promising adsorbent in water treatment field.

3.7. Adsorption mechanism

The FTIR spectroscopy for the characterization of MIEX resin before and after adsorption are shown in Fig. 7. Both types of MIEX resin exhibited similar characteristic peaks over the spectrum ranging from 500 to 4000 cm^{-1}, which indicates that the TBP adsorption does not change the basic structure of the MIEX, consistent with the result of SEM images in Fig. 8. There is no obvious visible change in the surface of MIEX resin before and after adsorption. The main functional groups and the corresponding infrared bands

were shown in Table 5. The sorption peak of C=O at 1720 cm^{-1} became weaken after adsorption, which may result from the formation of hydrogen bonds between C=O and water molecule [62–64]. The fingerprint region, sorption peaks at 1558 cm^{-1}, appeared after the adsorption, which represented the C=C groups in TBP benzene ring. Therefore, the adsorption of TBP on MIEX resin mainly depended on the hydrophobic interaction of the benzene ring and hydrogen bonds [65,66].

3.8. Regeneration and reusability

In order to make the sorption process viable, efficient regeneration and reuse test is necessary. For this purpose, MIEX resin saturated with TBP was regenerated by 1 M different regenerant solutions, including DI water, sodium chloride, hydrogen chloride and sodium hydroxide. After regeneration, MIEX resin was reconditioned using DI water to remove the excess regenerants. The performance of the regenerated resin was evaluated over three successive cycles. Reusability efficiency of MIEX resin for TBP adsorption is shown in Fig. 9. The highest TBP removal efficiency was near 90%, and others ranged from 80% to 90%. Each regenerant had an excellent regeneration capacity for MIEX resin, especially the sodium hydroxide. This demonstrated that MIEX resin had high reusability and was a perfect sorbent for TBP removal from water.

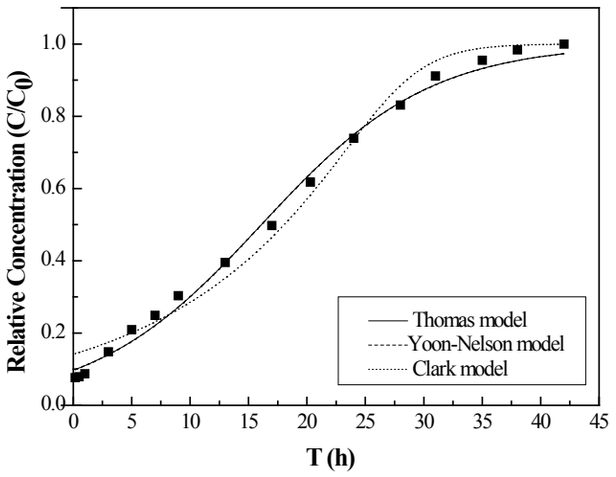

Fig. 6. Breakthrough curves of TBP onto MIEX resin (T = 298 K; TBP = 2.0 mg/L; pH = 7.80; flow rate = 1.0 mL/min). The solid lines represent non-linear curve fitting by Thomas model; the dash lines are the curve fitting by Yoon-Nelson model; the dot lines are the curve fitting by Clark model.

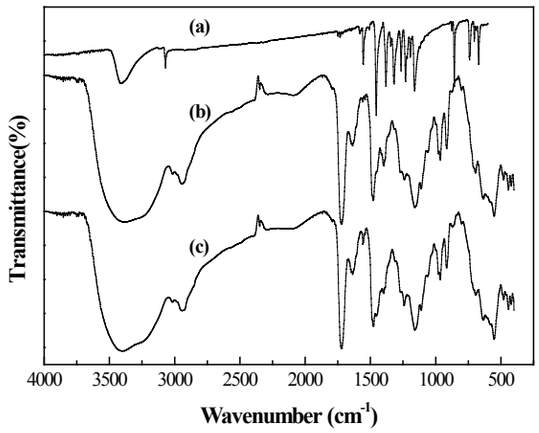

Fig. 7. FTIR spectra of (a) TBP, (b) MIEX before adsorption, and (c) after adsorption.

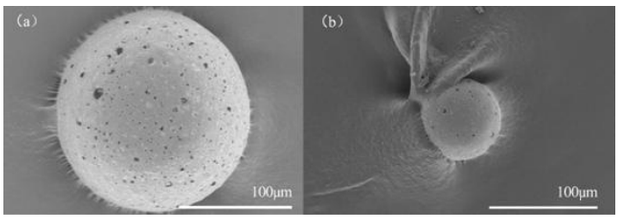

Fig. 8. The SEM image of MIEX resin before (a) and after (b) adsorption.

Table 5
FT-IR spectra characteristics of MIEX resin before and after TBP adsorption

Adsorption band/cm^{-1}		Assignment
Before adsorption	After adsorption	
3387	3403	Bonded -OH groups
3014	3016	Benzene C-H stretching
2944	2943	$-CH_2$ groups connected to benzene ring
1720	1720	C=O groups
1636–1478	1636–1477	Benzene ring skeleton stretching
1398	1395	$-CH_3$ groups
1160	1160	C-O groups

Table 4
Dynamic model fitting parameters of TBP sorption onto MIEX resin

Thomas model			Yoon–Nelson model			Clark model		
K_{TH}(mL/ (mg min))	q_0 (mg/g)	R^2	K (mg/mL)	T (1/h)	R^2	A	r(1/h)	R^2
0.069	23.77	0.995	0.138	16.10	0.995	43865.0	0.384	0.985

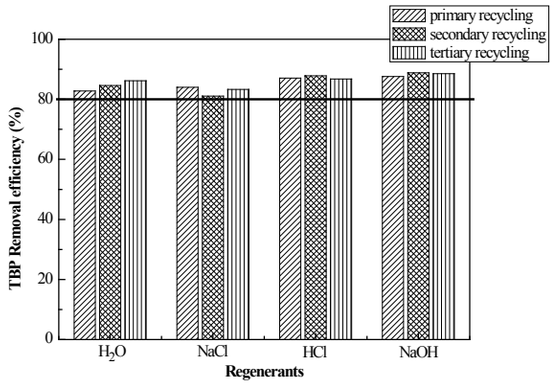

Fig. 9. Reusability efficiency of regenerated MIEX resin for three cycles (regenerant concentraton = 1 mol/L; T = 298 K; TBP = 2.0 mg/L; pH = 7.80; contact time = 10 h).

4. Conclusions

MIEX resin is an efficient material for TBP removal from aqueous solutions. The removal of TBP on MIEX resin is concentration dependent, and the uptake value increased with increasing initial TBP concentrations. The highest removal capacity of TBP on MIEX resin was obtained with the pH value of 7.80. The kinetics characteristics of TBP on MIEX resin can be well fitted by the pseudo-second-order model. The significant effect on TBP removal of coexisting anions kept the order: $SO_4^{2-} > HPO_4^{2-} > HCO_3^- > NO_3^-$. The same order of coexisting cations was given: $Mg^{2+} > Ca^{2+} > NH_4^+$. The equilibrium sorption of TBP on MIEX resin at 298 K can be well described by the Freundlich isotherm model. The uptake of TBP increased with the solution temperature increasing from 288 to 308K, and temperature had tiny influence on the removal of TBP. The thermodynamics studies showed that the sorption of TBP on MIEX resin was a thermodynamically feasible and spontaneously endothermic process naturally. The column test indicated MIEX could remove TBP efficiently under continuous flow with a maximum TBP adsorbed amount of 32.11 mg/g. The adsorption of TBP on MIEX resin mainly depended on the hydrophobic interaction of the benzene ring and hydrogen bonds. The results in this study show that MIEX has a good potential to be used as a sorbent for TBP removal from water.

Acknowledgments

This work was supported by the National Natural Science Foundation of China (No. 21776224), Key Projects in the National Science & Technology Pillar Program during the Twelfth Five-year Plan Period (2015BAE04B01)and National Water Pollution Control and Treatment Key Technologies RD Program(2015ZX07406-001).

References

[1] Q.Q. Zhu, M. Maeno,T. Miyamoto, M. Fukushima, Monopersulfate oxidation of 2,4,6-tribromophenol using an iron(III)-tetrakis (p-sulfonatephenyl) porphyrin catalyst supported on an ionic liquid functionalized Fe_3O_4 coated with silica, Appl. Catal. B-Environ., 163 (2015) 459–466.

[2] A.N. Halden, J.R. Nyholm, P.L. Andersson, H. Holbech, L. Norrgren, Oral exposure of adult zebrafish (Danio rerio) to 2,4,6-tribromophenol affects reproduction, Aquat. Toxicol., 100 (2010) 30–37.

[3] P. Andrewes, J.G. Bendall, G. Davey, R. Shingleton, A musty flavour defect in calcium caseinate due to chemical tainting by 2,4,6-tribromophenol and 2,4,6-tribromoanisole, Int. Dairy J., 20 (2010) 423–428.

[4] P. Dhiman, M. Naushad, K.M. Batoo, A. Kumar, G. Sharma, A. A. Ghfar, G. Kumar, M. Singh, Nano FexZn1–xO as a tuneable and efficient photocatalyst for solar powered degradation of Bisphenol A from water, J. Clean. Prod., 165 (2017) 1542–1556.

[5] T. Weidlich, L. Prokeš, D. Pospíšilová, Debromination of 2,4,6-tribromophenol coupled with biodegradation, Cent. Eur. J. Chem., 11 (2013) 979–987.

[6] J.Y. Li, X.Y. Long, H.X. Yin, J.Q. Qiao, H.Z. Lian, Magnetic solid-phase extraction based on a polydopamine-coated Fe_3O_4 nanoparticles absorbent for the determination of bisphenol A, tetrabromobisphenol A, 2,4,6-tribromophenol, and (S)-1,1′-bi-2-naphthol in environmental waters by HPLC, J. Sep. Sci., 39 (2016) 2562–2572.

[7] M. Igarashi,Q.Q. Zhu, M. Sasaki, R. Kodama, K. Oda, Catalytic oxidation of 2,4,6-tribromophenol using iron(III) complexes with imidazole, pyrazole, triazine and pyridine ligands, J. Mol. Catal. A-Chem., 413 (2016) 100–106.

[8] S. Fukuchi, R. Nishimoto, M. Fukushima, Q.Q. Zhu, Effects of reducing agents on the degradation of 2,4,6-tribromophenol in a heterogeneous Fenton-like system with an iron-loaded natural zeolite, Appl. Catal. B-Environ., 147 (2014) 411–419.

[9] C. Leonetti, C.M. Butt, K. Hoffman, M.L. Miranda, H.M. Stapleton, Concentrations of polybrominated diphenyl ethers (PBDEs) and 2,4,6-tribromophenol in human placental tissues, Environ. Int., 88 (2016) 23–29.

[10] S. Schafer, U. Bickmeyer, A. Koehler, Measuring Ca(2+)-signalling at fertilization in the sea urchin Psammechinus miliaris: alterations of this Ca(2+)-signal by copper and 2,4,6-tribromophenol, Comp. Biochem. Physc., 150 (2009) 261–269.

[11] X.L. Ma, D. Wu, L.M. Huang, Z.Y. Wu, S.C. Xiang, Sensing 2,4,6-tribromophenol based on molecularly imprinted technology, Monatsh. Chem., 146 (2014) 485–491.

[12] T. Weidlich, A. Krejčová, Hydrodebromination of 2,4,6-tribromophenol in aqueous solution using Devarda's alloy, Monatsh. Chem., 144 (2012) 155–162.

[13] B. Gao, L.F. Liu, J.D. Liu, F.L. Yang, Photocatalytic degradation of 2,4,6-tribromophenol on Fe_2O_3 or FeOOH doped ZnIn2S4 heterostructure: Insight into degradation mechanism, Appl. Catal. B-Environ., 147 (2014) 929–939.

[14] B. Gao, L.F. Liu, J.D. Liu, F.L. Yang, Photocatalytic degradation of 2,4,6-tribromophenol over Fe-doped ZnIn2S4: Stable activity and enhanced debrominationAppl. Catal. B-Environ., 129 (2013) 89–97.

[15] T. Yamada, Y. Takahama, Y. Yamada, Biodegradation of 2,4,6-tribromophenol by Ochrobactrum sp. strain TB01, Biosci. Biotechnol. Bioch., 72 (2008) 1264–1271.

[16] H.Y. Luo, X. Nie, G.Y. Li, J.K. Liu, T.C. An, Structural characterization and photocatalytic activity of hydrothermally synthesized mesoporous TiO_2 for 2,4,6-tribromophenol degradation in water, Chinese. J. Catal., 32 (2011) 1349–1356.

[17] Z.L. Li, N. Yoshida, A.J. Wang, J. Nan, B. Liang, Anaerobic mineralization of 2,4,6-tribromophenol to CO_2 by a synthetic microbial community comprising Clostridium, Dehalobacter, and Desulfatiglans, Bioresource. Technol., 176 (2015) 225–232.

[18] C. Donoso, J. Becerra, M. Martínez, N. Garrido, M. Silva, Degradative ability of 2,4,6-tribromophenol by saprophytic fungi Trametes versicolor and Agaricusaugustus isolated from chilean forestry, World. J. Microb. Bio., 24 (2007) 961–968.

[19] J. Aguayo, R. Barra, J. Becerra, M. Martínez, Degradation of 2,4,6-tribromophenol and 2,4,6-trichlorophenol by aerobic heterotrophic bacteria present in psychrophilic lakes, World. J. Microb. Bio., 25 (2008) 553–560.

[20] Q.Q. Zhu, Y. Mizutani, S. Maeno, R. Nishimoto, T. Miyamoto, Potassium monopersulfate oxidation of 2,4,6-tribromophenol catalyzed by a SiO_2-supported iron(III)-5,10,15,20-tetrakis (4-carboxyphenyl) porphyrin, J. Environ. Sci. Heal. A., 48 (2013) 1593–1601.
[21] M. Marková, P. Kučerová, J. Skopalová, P. Barták, Electrochemical oxidation of 2,4,6-tribromophenol in aqueous-alcoholic media, Electroanal., 27 (2015) 156–165.
[22] X. Lu, Y.S. Shao, N.Y. Gao, L. Ding, Equilibrium, thermodynamic, and kinetic studies of the adsorption of 2,4-dichlorophenoxyacetic acid from aqueous solution by MIEX resin, J. Chem. Eng. Data., 60 (2015) 1259–1269.
[23] M. Naushad, Z.A. Alothman, M.R. Awual, Adsorption of rose Bengal dye from aqueous solution by amberlite Ira-938 resin: kinetics, isotherms, and thermodynamic studies, Desal. Water. Treat., 57 (2016) 13527–13533.
[24] C. Mardones, D. Von Baer, A. Hidalgo, A. Contreras, C. Sepulveda, Determination of pentachlorophenol and tribromophenol in sawdust by ultrasound-assisted extraction and MEKC, J. Sep. Sci., 31 (2008) 1124–1129.
[25] A. Dabrowski, Z. Hubicki, P. Podkoscielny, E. Robens, Selective removal of the heavy metal ions from waters and industrial wastewaters by ion-exchange method, Chemosphere, 56 (2004) 91–106.
[26] A. Kumar, M. Naushad, A. Rana, ZnSe-WO3 nano-hetero-assembly stacked on Gum Ghatti for photo-degradative removal of Bisphenol A: Symbiose of adsorption and photocatalysis, Int. J. Biol. Macromol., 104 (2017) 1172–1184.
[27] Y.L. Tang, S. Liang, H.C. Guo, H.R. You, N.Y. Gao, Adsorptive characteristics of perchlorate from aqueous solutions by MIEX resin, Colloid. Surfaces. A., 417 (2013) 26–31.
[28] K. Watson, M.J. Farre, N. Knight, Enhanced coagulation with powdered activated carbon or MIEX secondary treatment: a comparison of disinfection by-product formation and precursor removal, Water. Res., 68 (2015) 454–466.
[29] M. Naushad, S. Vasudevan, G. Sharma, Adsorption kinetics, isotherms, and thermodynamic studies for Hg adsorption from aqueous medium using alizarin red-S-loaded amberlite IRA-400 resin, Desal. Water Treat., 2015 (2015) 1–9.
[30] T.V. Nguyen,R. Zhang, S. Vigneswaran, Removal of organic matter from effluents by magnetic ion exchange (MIEX®), Desalination, 276 (2011) 96–102.
[31] R. Zhang, S. Vigneswaran, H.H. Ngo, Magnetic ion exchange (MIEX®) resin as a pre-treatment to a submerged membrane system in the treatment of biologically treated wastewater, Desalination, 192 (2006) 296–302.
[32] L. Ding, X. Lu, H. Deng H, Adsorptive removal of 2,4-dichlorophenoxyacetic acid (2,4-D) from aqueous solutions using MIEX resin, Ind. Eng. Chem. Res., 51 (2012) 11226–11235.
[33] X. Zhang, X. Lu, S. Li, Investigation of 2,4-dichlorophenoxyacetic acid adsorption onto MIEX resin: Optimization using response surface methodology, J. Taiwan. Inst. Chem. E., 45 (2014) 1835–1841.
[34] L. Ding, C. Wu, H. Deng, Adsorptive characteristics of phosphate from aqueous solutions by MIEX resin, J. Colloid. Interf. Sci., 376 (2012) 224.
[35] K. Braun, L. Cruaux, R. Fabris, J. Morran, L. Ho, Comparison of coagulation and MIEX pre-treatment processes for bacterial and turbidity removal, utilizing real-time optical monitoring techniques, Environ. Technol., 35 (2014) 1038–1045.
[36] J. Xu, W.Y. Xu, D.S. Wang, G.Q. Sang, X.S. Yang, Evaluation of enhanced coagulation coupled with magnetic ion exchange (MIEX) in natural organic matter and sulfamethoxazole removals: The role of Al-based coagulant characteristic, Sep. Purif. Technol., 167 (2016) 70–78.
[37] H.C. Kim, High-rate MIEX filtration for simultaneous removal of phosphorus and membrane foulants from secondary effluent, Water. Res., 69 (2015) 40–45.
[38] E.R. Kenawy, A.A. Ghfar, M. Naushad, Efficient removal of Co(II) metal ion from aqueous solution using cost-effective oxidized activated carbon: Kinetic and isotherm studies, Desal. Water. Treat., 70 (2017) 220–226.
[39] C.M. Futalan, C.C. Kan, M.L. Dalida, C. Pascua, M.W. Wan, Fixed-bed column studies on the removal of copper using chitosan immobilized on bentonite, Carbohyd. Polym., 83 (2011) 697–704.
[40] Z. Aksu, F. Gönen, Biosorption of phenol by immobilized activated sludge in a continuous packed bed: prediction of breakthrough curves, Process. Biochem., 39 (2004) 599–613.
[41] S.H. Chen, Q.Y. Yue, B.Y. Gao, Q. Li, X. Xu, Adsorption of hexavalent chromium from aqueous solution by modified corn stalk: a fixed-bed column study, Bioresour. Technol., 113 (2012) 114–120.
[42] A.A. Alqadami, N. Mu, M.A. Abdalla, Adsorptive removal of toxic dye using Fe_3O_4–TSC nanocomposite: equilibrium, kinetic, and thermodynamic studies, J. Chem. Eng. Data., 61 (2016) 3806–3813.
[43] L. Ding, H.P. Deng, C. Wu, X. Han, Affecting factors, equilibrium, kinetics and thermodynamics of bromide removal from aqueous solutions by MIEX resin, Chem. Eng. J., 181 (2012) 360–370.
[44] L. Ding, C. Wu, H.P. Deng, X.X. Zhang, Adsorptive characteristics of phosphate from aqueous solutions by MIEX resin, J. Colloid. Interf. Sci., 376 (2012) 224–232.
[45] J.N. Wang, A.M. Li, L. Xu, Y. Zhou, Adsorption of tannic and gallic acids on a new polymeric adsorbent and the effect of Cu(II) on their removal, J. Hazard. Mater., 169 (2009) 794–800.
[46] L. Zu, G.Y. Li, T.C. An, P.K. Wong, Biodegradation kinetics and mechanism of 2,4,6-tribromophenol by Bacillus sp. GZT: a phenomenon of xenobiotic methylation during debromination, Bioresource. Technol., 110 (2012) 153–159.
[47] L. Zu, G.Y. Li, J.B. An, J.J. Li, T.C. An, Kinetic optimization of biodegradation and debromination of 2,4,6-tribromophenol using response surface methodology, Int. Biodeter. Biodegr., 76 (2013) 18–23.
[48] L. Ding, B. Du, G. Luo, H.P. Deng, Adsorption of bromate from emergently polluted raw water using MIEX resin: equilibrium, kinetic, and thermodynamic modeling studies, Desal. Water. Treat., 56 (2014) 2193–2205.
[49] Y.P. Zhu, N.Y. Gao, Q.F. Wang, X.Y. Wei, Adsorption of perchlorate from aqueous solutions by anion exchange resins: Effects of resin properties and solution chemistry, Colloid. Surfaces. A., 468 (2015) 114–121.
[50] H. Kuramochi, K. Kawamoto, S.L. Sakai, Effects of pH on the water solubility and 1-octanol-water partition coefficient of 2,4,6-tribromophenol, J. Environ. Monitor., 10 (2008) 206–210.
[51] M.L. Wang, Y.M. Hsieh, C.W. Chang, A kinetic study of phase transfer catalyzed benzylation of 2,4,6-tribromophenol in liquid-liquid two-phase solution, Chem. Eng. Commun., 198 (2011) 939–956.
[52] Y.L. Tang, S.Y. Li, Y.H. Zhang, S.L. Yu, M. Martikka, Sorption of tetrabromobisphenol A from solution onto MIEX resin: Batch and column test, J. Taiwan. Inst. Chem. E., 45 (2014) 2411–2417.
[53] J.T. Huang, L. Alquier, J.P. Kaisa, G. Reed, T. Gilmor, Method development and validation for the determination of 2,4,6-tribromoanisole, 2,4,6-tribromophenol, 2,4,6-trichloroanisole, and 2,4,6-trichlorophenol in various drug products using stir bar sorptive extraction and gas chromatography-tandem mass spectrometry detection, J. Chromatogr. A., 1292 (2012) 196–204.
[54] M. Aeschbacher, C. Graf, R.P. Schwarzenbach, M. Sander, Antioxidant properties of humic substances, Environ. Sci. Technol., 46 (2012) 4916–4925.
[55] B.H. Hameed, A.A. Ahmad, Batch adsorption of methylene blue from aqueous solution by garlic peel, an agricultural waste biomass, J. Hazard. Mater., 164 (2009) 870– 875.
[56] R. Chen, Q. Yang, Y. Zhong, X. Li, Y. Liu, Sorption of trace levels of bromate by macroporous strong base anion exchange resin: Influencing factors, equilibrium isotherms and thermodynamic studies, Desalination, 344 (2014) 306–312.
[57] E. Pehlivan, S. Cetin, Sorption of Cr(VI) ions on two Lewatit-anion exchange resins and their quantitative determination using UV-visible spectrophotometer, J. Hazard. Mater., 163 (2009) 448–453.

[58] W.Q. Wang, M.Y. Li, Q.X. Zeng, Thermodynamics of Cr(VI) adsorption on strong alkaline anion exchange fiber, T. Nonferr. Metal. Soc., 22 (2012) 2831–2839.
[59] S. Kundu, A.K. Gupta, Analysis and modeling of fixed bed column operations on As(V) removal by adsorption onto iron oxide-coated cement (IOCC), J. Colloid. Interf. Sci., 290 (2005) 52–60.
[60] F.W. Sousa, A.G. Oliveira, J.P. Ribeiro, M.F. Rosa, D. Keukeleire, Green coconut shells applied as adsorbent for removal of toxic metal ions using fixed-bed column technology, J. Environ. Manage., 91 (2010) 1634–1640.
[61] M. Naushad, Surfactant assisted nano-composite cation exchanger: Development, characterization and applications for the removal of toxic Pb^{2+}, from aqueous medium, Chem. Eng. J., 235 (2014) 100–108.
[62] Y. Zhang, Y. Tang, S. Li, Sorption and removal of tetrabromobisphenol A from solution by graphene oxide, Chem. Eng. J., 222 (2013) 94–100.
[63] W.Q. Wang, Y.L. Ming, Q.X. Zeng, Thermodynamics of Cr(VI) adsorption on strong alkaline anion exchange fiber, T. Nonferr. Metal. Soc., 22 (2012) 2831–2839.
[64] M. Naushad, T. Ahamad, B.M. Al-Maswari, Nickel ferrite bearing nitrogen-doped mesoporous carbon as efficient adsorbent for the removal of highly toxic metal ion from aqueous medium, Chem. Eng. J., 330 (2017) 1351–1360.
[65] A.A. Alqadami, M. Naushad, Z.A. Alothman, Novel metal-organic framework (MOF) based composite material for the sequestration of U(VI) and Th(IV) metal ions from aqueous environment, Acs. Appl. Mater. Inter., 9 (2017) 36026–36037.
[66] G. Sharma, M. Naushad, A. Kumar, Efficient removal of Coomassie brilliant blue R-250 dye using starch/poly(alginic acid- cl -acrylamide) nanohydrogel, Process. Saf. Environ., 109 (2017) 301–310.